



HAL
open science

Modeling of a vibrating MEMS magnetometer partially covered with a ferromagnetic thin film

Thomas Perrier, Raphaël Levy, Patrick Kayser, Béatrice Verlhac, Johan Moulin

► **To cite this version:**

Thomas Perrier, Raphaël Levy, Patrick Kayser, Béatrice Verlhac, Johan Moulin. Modeling of a vibrating MEMS magnetometer partially covered with a ferromagnetic thin film. *Inertial Sensors* 2018, Mar 2018, COME, Italy. hal-01961024

HAL Id: hal-01961024

<https://hal.science/hal-01961024>

Submitted on 19 Dec 2018

HAL is a multi-disciplinary open access archive for the deposit and dissemination of scientific research documents, whether they are published or not. The documents may come from teaching and research institutions in France or abroad, or from public or private research centers.

L'archive ouverte pluridisciplinaire **HAL**, est destinée au dépôt et à la diffusion de documents scientifiques de niveau recherche, publiés ou non, émanant des établissements d'enseignement et de recherche français ou étrangers, des laboratoires publics ou privés.

Modeling of a vibrating MEMS magnetometer partially covered with a ferromagnetic thin film

Thomas Perrier, Raphaël Levy, Patrick Kayser,
Béatrice Verlhac
ONERA - The French Aerospace Lab
Châtillon, France
thomas.perrier@onera.fr

Johan Moulin
Nanoscience and Nanotechnology Center
Paris Saclay University
Orsay, France

Abstract— This paper describes a fully analytic model of sensitivity of a vibrating magnetometer partially covered with a ferromagnetic thin film. This model is based on the Rayleigh’s energetic method and is confirmed by Finite Element Method (FEM) and experimental measurements. Thereby, it is possible to optimize the position of the ferromagnetic thin film and find the best tradeoff between the sensitivity increase and the reduction of resonator energy losses to achieve better resolution.

Keywords—sensitivity modeling; magnetometer; MEMS; resonator; navigation

I. INTRODUCTION

Resonant micro-magnetometers have been developed during the last decade and have a wide range of applications [1]. Among these, magnetometers are increasingly used for indoor navigation in conjunction with low cost Inertial Measurement Units (IMUs), mainly to correct gyro drift over time and so acting as a heading reference [2]. More recent applications use magnetometers combined with IMUs in magneto-inertial navigation technique (MINAV) to measure the local distribution of the magnetic field and reach accurate motion estimation [3]. MEMS resonator based magnetometers are suitable for these applications due to low cost, small size and low power consumption. However, to be efficient in the most demanding applications, their resolution needs to be improved. For this purpose, vibrating beam magnetometers with ferromagnetic thin layer sputtered on the resonator seem to be a promising way [4], [5].

This kind of magnetometer uses the frequency shift of a resonator due to magnetic interaction between the ferromagnetic layer and the magnetic field applied to deduce the magnetic field value in the environment of the sensor. To optimize this magnetometer, a model is established to obtain the differential equation of the vibrating beam, with a thin ferromagnetic layer partially sputtered on it and subjected to a homogeneous magnetic field. Then it is solved by analogy with the Vibrating Beam Accelerometer (VBA) principle with the Rayleigh’s energetic method. Finally, an expression of the natural frequency of the beam as a function of the magnetic field applied is obtained, and the sensitivity of the sensor is deduced. In a second part, this model is validated by FEM simulations and compared with experimental measurements.

II. DIFFERENTIAL EQUATION OF MOTION OF THE VIBRATING MAGNETOMETER

A. Model presentation

Fig. 1 illustrates a bending clamped-free beam which models the magnetometer. The beam is a rectangular cross-section beam of width e , thickness h and length L . It vibrates in a flexural mode in the xy -plane with an amplitude $w(x,t)$. The magnetic thin film is supposed to act as a distributed torque along the main axis of the beam. In this first part, magnetic thin film covers integrally the top of the beam. Magnetization M_{mag} of the thin film is supposed to perfectly match the deformation of the beam. Equation resolution is made under Bernoulli’s assumptions: no warping and no rotation inertia of the cross-section, which supposed to have $L \gg e, h$. The main difference from the classical resolution of a bending beam comes from the distributed torque.

B. Differential equation of motion

Fig. 2 illustrates an elementary section of beam, where $Q(x)$, $M(x)$ and $\Gamma_{mag}(x)$ are respectively shear force, moment and elementary magnetic torque acting on the beam.

- Elementary magnetic torque is deduced from the classical magnetostatic interaction, considering small angles:

$$\Gamma_{mag} = -M_{mag} S_{mag} B \frac{\partial w}{\partial x} dx \quad (1)$$

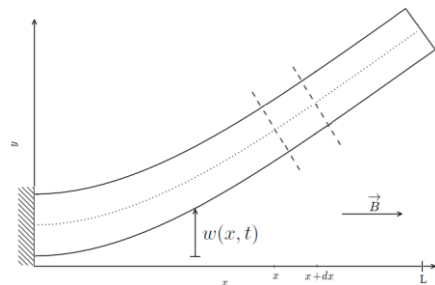


Fig. 1. Schematic view of a bending clamped-free beam

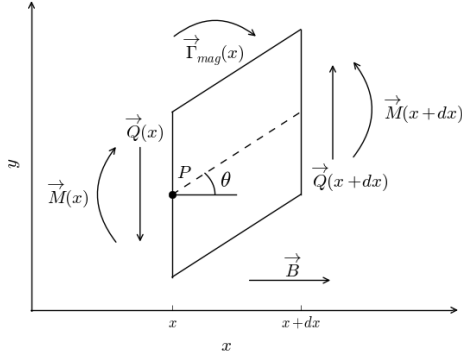


Fig. 2. Illustration of an elementary section of beam with forces and torques acting on it

where $S_{mag}=e.t$ is the cross-section area of the ferromagnetic thin film of thickness t .

- Forces acting on y-axis lead to:

$$\frac{\partial Q}{\partial x} = \rho S \frac{\partial^2 w}{\partial t^2} \quad (2)$$

where ρ is the density and S the cross-sectional area.

- Considering there is no rotation inertia (Bernoulli's assumption), moments acting on z-axis lead to:

$$\frac{\partial M}{\partial x} + Q - M_{mag} S_{mag} B \frac{\partial w}{\partial x} = 0 \quad (3)$$

- Knowing that $M(x,t) = EI \frac{\partial^2 w}{\partial x^2}$ for beam in flexion, differential equation of motion can be deduced from previous equations:

$$EI \frac{\partial^4 w}{\partial x^4} - M_{mag} S_{mag} B \frac{\partial^2 w}{\partial x^2} + \rho S \frac{\partial^2 w}{\partial t^2} = 0 \quad (4)$$

III. RESOLUTION OF THE DIFFERENTIAL EQUATION

It is interesting to note that the differential equation (4) is exactly the same as the one governing Vibrating Beam Accelerometers (VBA) subjected to an axial force [6] where the term $M_{mag} S_{mag} B$ acts as an equivalent axial force. This term will be called F_{mag} thereafter.

A. Solution without magnetic field

A solution of (4) is found by using the technique of separation of variables:

$$w(x,t) = Y(x).T(t) \quad (5)$$

Hence, two ordinary differential equations are obtained; their solutions are well-known in the case without magnetic

field. $T(t)$ is a harmonic function and $Y(x)$ is expressed in the clamp-free case as:

$$Y_n(x) = C[\sin b_n x - \sinh b_n x + K_n(\cos b_n x - \cosh b_n x)] \quad (6)$$

with:

$$b_n = \frac{\alpha_n/L}{\sin \alpha_n - \sinh \alpha_n} \quad (5)$$

where α_n is a numerical constant depending on the mode number. The natural frequency without magnetic field is then:

$$f_{n,0} = \frac{\alpha_n^2}{2\pi\sqrt{12}} \sqrt{\frac{E}{\rho} \frac{e}{L^2}} \quad (7)$$

B. Solution for fully covered beam

In this case two ways are possible to solve equation 4. The first uses the same method than previously and solves a characteristic equation for the system. This method is used for example in [6]. However, to avoid lengthy analytical derivations, it is easier to use Rayleigh's energetic method, particularly for the partially covered beam. This method is based on the equality between the maximum of potential and kinetic energy, in the assumption there is no energy dissipation mechanism.

The maximum kinetic and flexural energy are:

$$E_{c,n} = \frac{\omega_{n,B}^2 \rho e h}{2} \int_0^L Y_n^2(x) dx \quad (8)$$

$$E_{p,flexion,n} = \frac{EI}{2} \int_0^L \left(\frac{\partial^2 Y_n}{\partial x^2} \right)^2 dx$$

The potential torque energy is obtained by integration of an elementary variation of potential energy $dE_p = T(x)d\theta$. Where $T(x)$ is the torque applied at point x on the beam. As the problem is in the small deformation assumption, the maximum torque potential energy is then:

$$E_{p,mag,n} = \frac{F_{mag}}{2} \int_0^L \left(\frac{\partial Y_n}{\partial x} \right)^2 dx \quad (9)$$

With the assumptions that the deformation of a beam is not changed by application of a small torque on it, previous integrals can be solved by using (6). In the case without magnetic field, natural frequency has the same expression than in (7) with:

$$\alpha_n^2 = L^2 \frac{\int_0^L (Y_n^{(2)})^2 dx}{\int_0^L (Y_n)^2 dx} \quad (10)$$

Considering the magnetic field, natural frequency is modified and is expressed as:

$$f_{n,B} = f_{n,0} \sqrt{1 + \frac{\beta_n F_{mag}}{4\pi^2 L^2 \rho e h f_{n,0}^2}} \quad (11)$$

where:

$$\beta_n = L^2 \frac{\int_0^L (Y_n^{(1)})^2 dx}{\int_0^L (Y_n)^2 dx} \quad (12)$$

Finally, $f_{n,B}$ is expressed as a Taylor series around $B=0$:

$$f_{n,B} = f_{n,0} + K_1 B + K_2 B^2 + K_3 B^3 + o(B^3) \quad (13)$$

where:

$$\begin{cases} K_1 = \frac{\sqrt{3} \beta_n t M_{mag}}{2\pi \alpha_n^2 e h \sqrt{E\rho}} \\ K_2 = -\frac{1 K_1^2}{2 f_{n,0}} \\ K_3 = \frac{1 K_1^3}{2 f_{n,0}^2} \end{cases} \quad (14)$$

In (14), K_1 is the sensitivity of the beam to the magnetic field applied. The stronger the field the larger the frequency shift. The others terms characterize non-linearity that can appear under high magnetic field. Tab. 1 summarizes numerical values used in (14). It is interesting to note that the sensitivity is almost identical for all modes used. As ultimate resolution needs the lowest natural frequency [5], the best mode for use as magnetometer is the fundamental.

C. Solution for partially covered beam

For a partially covered beam, the only difference is in the expression of the potential energy of the magnetic torque. Considering the most general case with a ferromagnetic

TABLE I. NUMERICAL VALUES OF CONSTANTS USES IN FREQUENCY AND SENSITIVITY EXPRESSIONS OF A CLAMP-FREE BEAM FOR THESE FIRST FLEXURAL MODES

Mode	1	2	3
α_n	1.875104	4.694091	7.854757
β_n	4.647793	32.41735	77.29909
$\gamma_n = \beta_n / \alpha_n^2$	1.321892	1.471209	1.252878

layer between x_1 and x_2 ($0 < x_1 < x_2 < L$):

$$E_{p,mag,n} = \frac{F_{mag}}{2} \int_{x_1}^{x_2} \left(\frac{\partial Y_n}{\partial x} \right)^2 dx \quad (15)$$

It is easier to solve it using the linearity of the integral:

$$I_n(x) = \frac{1}{a_{1,n}^2 b_n} \int_0^x \left(\frac{\partial Y_n}{\partial x'} \right)^2 dx' \quad (15)$$

with (6) an analytical solution can be obtained for (15):

$$I_n(x) = \begin{aligned} & (K_n^2 + 1) \sinh b_n x [\cosh b_n x - 2 \cos b_n x] \\ & + (K_n^2 - 1) \sin b_n x [2 \cosh b_n x - \cos b_n x] \\ & + 2K_n [\cosh b_n x - \cos b_n x]^2 + 2b_n x \end{aligned} \quad (17)$$

Finally, the sensitivity can be expressed as:

$$K_{I,partial} = J_n(x_1, x_2) \cdot K_{I,full} \quad (15)$$

with:

$$J_n(x_1, x_2) = \frac{I_n(x_2) - I_n(x_1)}{I_n(L)} \quad (15)$$

IV. MODEL VALIDATIONS

A. FEM validations

A FEM model using OOFELIE::Multiphysics solver has been developed by Open Engineering to model an elementary torque applied on elements proportionally to local deformation. Modal simulations with and without torques applied allow deducing frequency sensitivity to magnetic field for a resonator shape.

Simulations on simple beams are in very good agreement with analytical model. As shown in Fig. 3, using surface elements in FEM model, sensitivity perfectly match the analytical model. However, using volume elements for the

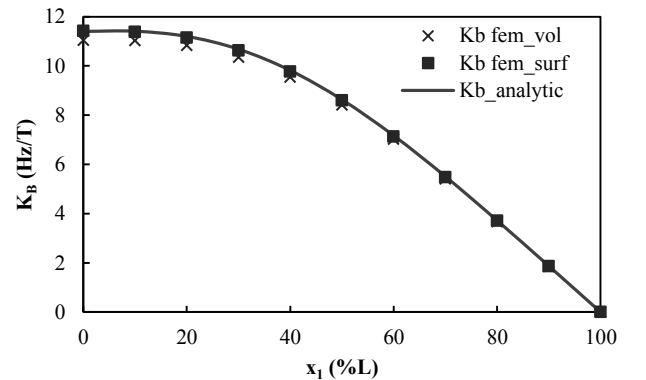


Fig. 3. Sensitivity versus x_1 ($x_2=L$) for a Quartz beam of width $70\mu\text{m}$, thickness $30\mu\text{m}$ and length $1400\mu\text{m}$.

torque allows considering the thin film's mass, that is why a small difference appears between results. So, analysis with volume elements is a more realistic model which will be more accurate in case where the thin film's mass is not negligible, at the price of a larger computation time.

B. Experimental validations

Vibrating beam magnetometers presented here are made by chemical etching of z-cut quartz wafer. To reduce anchor losses and thus increase Q factor of the resonator, prototypes have a tuning-fork shape instead of a simple beam. Gold actuation electrodes are at bottom and allow actuating piezoelectrically the tuning-fork at its first flexural mode. A NiCo ferromagnetic thin film is sputtered on top of the beam and magnetized along the main axis of the beam (Fig. 4). Remanent magnetization of NiCo film is about $1e6$ A/m [5]. Microscopic observations show the thin film forms a conformal coating on top and lateral faces of the beam, consequently this additional ferromagnetic material must be considered in the sensitivity calculations. The measuring bench uses a solenoid as magnetic field source, an oscillator circuit to sustain resonator's oscillations and a frequency counter. Frequency measures are made under a high vacuum ($<10^{-3}$ mbar) to limit viscous damping. For different magnetic field values applied, the resonator frequency is read, which makes it possible to deduce the sensitivity. Results are summarized in Table 2 and show a very good agreement between measures and analytic model.

CONCLUSION AND PERSPECTIVES

The analytical model presented in this paper makes it possible to calculate the sensitivity of a vibrating beam magnetometer partially covered with a ferromagnetic thin film. FEM analysis and experimental measurements on a small number of prototypes allow a first validation of this model. A larger number of prototypes is in manufacturing and measurements will be available soon. This will be useful in a

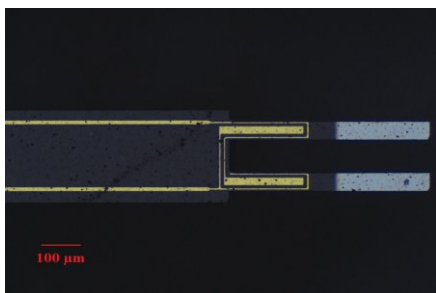


Fig. 4. Illustration of a tuning-fork quartz magnetometer with $50\mu\text{m}$ width and $500\mu\text{m}$ length. Actuation electrodes are in yellow, NiCo ferromagnetic layers are in grey.

TABLE II. SUMMARY OF SENSITIVITY MEASUREMENTS AND COMPARISON WITH ANALYTIC AND VOLUME FEM MODELS

Thin film thickness (nm)	Beam e/h/L (μm)	Position of the film x_1/x_2	Sensitivity (Hz/T)		
			Experiment	Analytic	FEM
200	80/30/1000	0 – L	5	4	4
500	50/30/800	0 – L	17	18	16
500	70/30/1400	0 – L	12	11	10
1000	70/30/1400	0 – L	19	22	20
200	150/30/1500	0.55L – L	0.8	1.0	0.9
500	150/30/1500	0.55L – L	1.8	2.4	2.2

second time to optimize the resolution of the vibrating beam magnetometer. Indeed, constrains in the ferromagnetic film generate viscoelastic losses which decrease the quality factor [5]. Thus, an optimization of the position of the film is necessary to maximize the quality factor of the resonator without too much reducing the sensitivity of the sensor. This will allow to obtain the best resolution for a vibrating beam magnetometer.

ACKNOWLEDGMENT

This work was supported by the French ANR program Astrid (ANR-15-ASTR-0012) led by the French Ministry of Army (DGA), under the contract "MAGRIT".

REFERENCES

- [1] A. L. Herrera-May, L. A. Aguilera-Cortés, P. J. García-Ramírez, N. B. Mota-Carrillo, W. Y. Padrón-Hernández, and E. Figueras, "Development of Resonant Magnetic Field Microsensors: Challenges and Future Applications," in *Microsensors*, InTech, 2011.
- [2] D. Gebre-Egziabher, G. H. Elkaim, J. D. Powell, and B. W. Parkinson, "A gyro-free quaternion-based attitude determination system suitable for implementation using low cost sensors," in *IEEE 2000. Position Location and Navigation Symposium (Cat. No.00CH37062)*, 2000, pp. 185–192.
- [3] E. Dorveaux, T. Boudot, M. Hillion, and N. Petit, "Combining inertial measurements and distributed magnetometry for motion estimation," in *Proceedings of the 2011 American Control Conference*, 2011, pp. 4249–4256.
- [4] J. W. van Honschoten, W. W. Koelmans, S. M. Konings, L. Abelmann, M. Elwenspoek, J. van Honschoten, W. W. Koelmans, and J. W. van Honschoten, "Nanotesla torque magnetometry using a microcantilever," *Proc. Eurosensors XXII, Eur. Conf. Solid-State Transducers*, pp. 597–600, 2008.
- [5] R. Levy, T. Perrier, P. Kayser, B. Bourgeteau, and J. Moulin, "A micro-resonator based magnetometer," *Microsyst. Technol.*, Jan. 2016.
- [6] Institute of Electrical and Electronics Engineers, "IEEE Standard Specification Format Guide and Test Procedure for Linear, Single-Axis, Non-Gyroscopic Accelerometers," no. September. p. 249, 1998.